Turkish Journal of Earth Sciences (Turkish J. Earth Sci.), Vol. 21, 2012, pp. 1–17. Copyright ©TÜBİTAK
doi:10.3906/yer-1006-26 First published online 02 February 2011

Dating Subduction Events in East Anatolia, Turkey

ROLAND OBERHÄNSLI[1], ROMAIN BOUSQUET[1], OSMAN CANDAN[2] & ARAL I. OKAY[3]

[1] Institute of Earth- & Environmental Sciences, Potsdam University, Karl-Liebknecht-Strasse 24, 14476 Potsdam, Germany (E-mail: roob@geo.uni-potsdam.de)
[2] Dokuz Eylül University, Engineering Faculty, Department of Geological Engineering, Buca, TR–35160 İzmir, Turkey
[3] İstanbul Technical University, Eurasia Institute of Earth Sciences, Maslak, TR–34469 İstanbul, Turkey

Received 29 June 2011; revised typescript received 08 January 2011; accepted 23 January 2011

Abstract: Metamorphic studies in the cover sequences of the Bitlis complex allow the thermal evolution of the massif to be constrained using metamorphic index minerals. Regionally distributed metamorphic index minerals such as glaucophane, carpholite, relics of carpholite in chloritoid-bearing schists and pseudomorphs after aragonite in marbles record a LT–HP evolution. This demonstrates that the Bitlis complex was subducted and stacked to form a nappe complex during the closure of the Neo-Tethys. During late Cretaceous to Cenozoic evolution the Bitlis complex experienced peak metamorphism of 1.0–1.1 GPa at 350–400°C. During the retrograde evolution temperatures remained below 460°C. $^{39}Ar/^{40}Ar$ dating of white mica in different parageneses from the Bitlis complex reveals a 74–79 Ma (Campanian) date of peak metamorphism and rapid exhumation to an almost isothermal greenschist stage at 67–70 Ma (Maastrichtian). The HP Eocene flysch escaped the greenschist facies stage and were exhumed under very cold conditions. These single stage evolutions contrast with the multistage evolution reported further north from the Amassia-Stepanavan Suture in Armenia. Petrological investigations and isotopic dating show that the collision of Arabia with Eurasia resulted in an assemblage of different blocks derived from the northern as well as from the southern plate and a set of subduction zones producing HP rocks with diverse exhumation histories.

Key Words: Bitlis complex, HP metamorphism, Ar dating, geodynamic evolution of SE Anatolia, subduction history

Doğu Anadolu'da (Türkiye) Yitim Olaylarının Yaşlandırılması

Özet: Bitlis Kompleksi'nin örtü serilerinde gerçekleştirilen indeks minerallere dayalı metamorfizma çalışması Masif'in termal evriminin ortaya konmasını mümkün kılmıştır. İyi korunmuş glaukofan ve karfolitin yanı sıra kloritoid içeren şistlerdeki karfolit kalıntıları ve mermerlerde aragonitten dönüşme kalsitin varlığı DS–YB koşullarındaki bir metamorfizmayı tanımlamaktadır. Bu bulgular, Bitlis Kompleksi'nin Neo-Tetis'in kapanması sırasında yitim zonunda derin gömülmeye uğrayarak nap yığını yapısı kazandığını göstermektedir. Petrolojik verilere dayanarak, Geç Kretase–Senozoyik zaman aralığında Bitlis Kompleksi'nde söz konusu metamorfizmanın zirve koşulları 350–400°C sıcaklık ve 1.0–1.1 GPa basınç olarak belirlenmiştir. Geri dönüşüm sürecinde ise sıcaklık 460°C nin altında kalmıştır. Farklı parajenezlerdeki beyaz mikaların $^{39}Ar/^{40}Ar$ yöntemiyle yaşlandırılmasına dayalı olarak, Bitlis Kompleksi'ndeki metamorfizmanın zirve koşullarının yaşı 74–79 My (Kampaniyen) olarak belirlenmiştir. Yaklaşık eş sıcaklık koşullarında hızlı yüzeylemeyi tanımlayan yeşilşist üzerlemesinin yaşı ise 67–70 My (Maastihtiyen) dır. YB Eosen filişi yeşilşist fasiyesi üzerlemesinden kaçmış ve çok soğuk koşullarda yüzeylemiştir. Bu tek aşamalı evrimler, daha kuzeyde, Ermenistan'da Amassia-Stepanavan kenetinde belirlenen çok evreli gelişimle uyuşmamaktadır. Petrolojik araştırmalar ve izotopik yaş verileri, Arabistan levhası ile Avrasya'nın çarpışmasının kuzey ve güneyden türeyen farklı blokların bir araya gelmesine neden olduğunu ve bu süreç içerisinde farklı yüzeyleme tarihçelerine sahip YB metamorfizması kayaları türeten bir dizi yitim zonunun geliştiğini göstermektedir.

Anahtar Sözcükler: Bitlis Kompleksi, YB Metamorfizması, Ar yaşlandırması, GD Anadolu'nun jeodinamik evrimi, yitim tarihçesi

Introduction

This paper reports petrological and isotopic data gathered in the context of the Middle East Basin Evolution program MEBE sponsored by a multinational energy consortium. The aim is to add knowledge about the structural and thermal evolution of the eastern Bitlis complex and the geodynamic evolution related to the collision of Arabia with Eurasia. Göncüoğlu and co-workers previously mapped part of the Bitlis metamorphic complex, between Bitlis and Muş (Göncüoğlu & Turhan 1984, 1992, 1997). A study of the lithostratigraphy and the Alpine metamorphic evolution of the Eastern Bitlis complex revealed a high-pressure low temperature evolution (Oberhänsli *et al.* 2010). In this paper we report isotopic ages and the geodynamic consequences of high-pressure from metasediments and mafic metamorphic rocks from the Palaeozoic to Mesozoic sedimentary cover of the Bitlis complex.

Geological Setting of South-Eastern Turkey

In southeast Anatolia the Bitlis complex forms an arcuate metamorphic belt, about 30 km wide and 500 km long, rimming the Arabian Platform (Figure 1a). Along the northern front of the Arabian plate a set of collisional autochthonous and allochthonous structures and units include from S to N: the Great Zap anticlinorium, the Eocene olistostromes of the Hakkari complex overlain by Cretaceous mélanges of the Yüksekova complex, the metamorphic rocks of the Bitlis complex and the Quaternary volcanics north of Lake Van. The Bitlis metamorphic complex comprises Precambrian to Cretaceous rocks and is covered by Tertiary sediments and Quaternary volcanics in the north, while to the south it overlies the Eocene to Miocene Hakkari and Maden complexes (Baykan, Ziyaret and Urse formations, S of Bitlis), as well as the sediments of the northern margin of the Arabian autochthon (e.g., Yılmaz 1993). East of the Bitlis complex the Cretaceous Yüksekova complex overlies the Tertiary units. An early description by Tolun (1953) interpreted the metamorphic rocks of the Bitlis complex as forming the basement of the region. Göncüoğlu and Turhan (1984), and Kellogg (1960) interpreted the Bitlis metamorphics as equivalents of the Arabian autochthonous succession and assigned a Devonian–Upper Cretaceous depositional age to the metasediments. Further detailed descriptions of the Bitlis complex were given by Horstink (1971), Boray (1975), Hall (1976), Yılmaz (1978), Çağlayan *et al.* (1984), and Sungurlu (1974).

Şengör & Yılmaz (1981) and Keskin (2003) proposed various geodynamic interpretations. New geophysical data on the East Anatolian plateau are interpreted as revealing an upwelling of asthenospheric mantle north of the Bitlis complex (Zor *et al.* 2003; Gök *et al.* 2007).

The Eastern Bitlis Complex

At the eastern limits of the Bitlis complex a cross section from Van to Hakkari cuts Cretaceous and Tertiary sequences. Oligo–Miocene sediments near Van exhibit neotectonic structures typical for the whole region. Tertiary and recent deformation led to faulting and block tilting. These Oligo–Miocene sediments overlie the eastern extensions of the Bitlis complex and are tectonically overlain by Cretaceous ophiolitic coloured mélange, with a serpentinitic and shaly matrix containing large limestone blocks (Yüksekova formation). To the south near the Hakkari - Yüksekova junction, the Yüksekova formation tectonically overlies the Eocene Hakkari complex, which in turn overrides the Eocene Urse formation. All these imbricated tectonic complexes are also exposed along the major thrust fault bounding the Arabian platform (Figure 1a).

The lithostratigraphic sequence of the Bitlis complex is given in a generalised columnar section based on Turhan and Göncüoğlu (1984) and contains (Figure 1b) from bottom to top:

1. Pre- to Infra-Cambrian augen gneiss with biotite, muscovite, amphibole; amphibolites and garnet-amphibolites with eclogite relics (Okay *et al.* 1985) and schists containing biotite, muscovite, garnet and amphibole, which are the oldest portions of the Bitlis complex.
2. Devonian metaconglomerates, metaquartzites and greenschists with limestone interlayers, reef limestones and albite-chlorite-actinolite-chloritoid schists of probable volcanogenic origin unconformably overlying the Infra-Cambrian. They grade upward into volcanoclastic sequences consisting of felsic metavolcanics and metatuffs.

3. Both formations are intruded by a metagranite. This metagranite is not affected by the Pre-Cambrian regional metamorphism (Göncüoğlu 1984). Its Late Cretaceous age (Helvacı & Griffin 1984) is poorly constrained.
4. A Lower Permian limestone formation, consisting of recrystallized limestones interbedded with chloritoid schists and graphite schists unconformably overlies all three units: Pre-Cambrian crystalline basement, Devonian metaclastics and metavolcanics as well as the metagranite. This sequence grades into calc-schists and thin-bedded recrystallized limestones.
5. On top of these thinly bedded metacarbonates an Upper Permian sequence of coarsely bedded recrystallized limestones with interlayers of calc-schists, metasandstones and chlorite schists was deposited.
6. Triassic rocks complete the section of the Bitlis complex. They consists of recrystallized limestones and calc-schists grading upward into metashales, metatuffs, metadiabases and metabasalts and finally metaconglomerates, metamudstones and shales, indicating a drastic change in depositional conditions. The Permo–Triassic formations contain metaquartz porphyries. They are interpreted as resulting from the opening of the Tethys Ocean.

Basement rocks in the central Bitlis complex contain kyanite-eclogites within garnet-mica schists and gneisses (Okay *et al.* 1985). P-T estimates indicate temperatures between 600 and 650°C at 1.0 to 2.0 GPa. Based on lithostratigraphic observations a Panafrican age was assumed for these eclogites (Göncüoğlu & Turhan 1997). For eclogite remnants in the basement of the eastern Bitlis complex a pressure of 1.9–2.4 GPa and temperature of 480–540°C was deduced (Oberhänsli *et al.* 2010), P-T conditions somewhat cooler than those estimated by Okay *et al.* (1985) for the Gablor mountains south of Muş. As yet, no age determinations for the basement eclogites exist.

The NE contact of the Bitlis complex near Gevaş (Figure 1a) is of special interest. There, an ophiolitic mélange is exposed with a serpentinitic matrix containing blocks of gabbro, basalt, chert, limestones with rudists of Arabian facies affinity (Özer 2005), and radiolarites. This area was reported as an ophiolite with a metamorphic sole (Yılmaz 1978). This unmetamorphosed mélange clearly dips southwards below the Bitlis complex. Listwaenites (Çolakoğlu 2009) and strongly deformed and brecciated rocks of both complexes, ophiolitic mélange and overlying Bitlis metamorphics, dominate the contact. Between the Permian Bitlis marbles and the ophiolite complex a conspicuous Triassic sequence (Tütü formation) contains relics of carpholite fibres. This clearly indicates low-grade high-pressure metamorphism and not a HT metamorphic sole. East of Gevaş radiolarites of the mélange complex are in steep contact with mylonitic marbles. These marble-mylonites are part of a metamorphic marble-schist sequence that typically occurs at the base of the Triassic series. Metapelitic layers contain white mica and chloritoid. Mafic layers are composed of intercalated greenschists and blueschists containing albite, chlorite, glaucophane and epidote (Çolakoğlu 2009; Oberhänsli *et al.* 2010). The schist-marble sequence has conformable contacts with Megalodon-bearing Triassic massive grey marbles.

In the Çatak valley (easternmost Bitlis complex, Figure 1a) the Palaeozoic marbles show strong cataclastic disruption and earlier ductile folding. Intercalated with these Palaeozoic marbles, a sequence of black to silvery schists with mafic layers occurs. In these schists (Figure 2a) Fe-Mg-carpholite relics record subduction-related metamorphic conditions. Fe,Mg-carpholite has mostly reacted to form chloritoid (Figure 2b, c) and quartz, but rarely kyanite. Associated mafic rocks contain glaucophane. Strongly folded Palaeozoic to Permo–Triassic marbles form the southern frontal part of the Bitlis complex. Along the Çatak River, these marbles contain fresh Fe-Mg-carpholite but no chloritoid (Figure 2d).

Metamorphism

The bulk of the eastern Bitlis complex, especially its basement, is made up of garnet-biotite mica-schists and biotite mica-schists with HP mineral paragenesis only locally preserved. Mafic rocks correspondingly

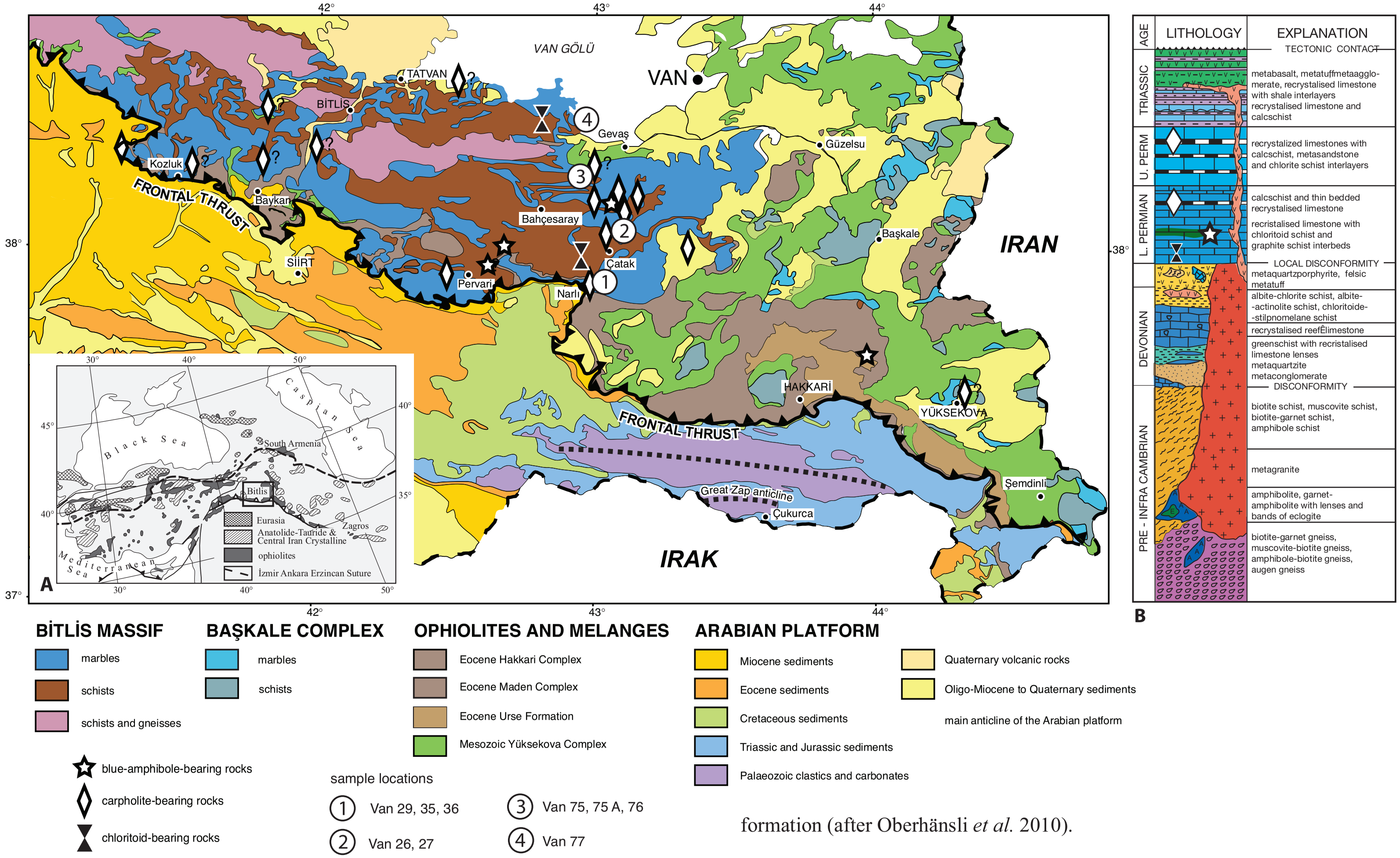

formation (after Oberhänsli *et al.* 2010).

Figure 1. **(A)** Geological map of the Eastern Bitlis complex (modified after MTA 1: 5000000 maps Cizre and Van). **(B)** Lithologic column adapted from Göncüoğlu & Turhan (1984) Mineral distribution shows blue amphibole and carpholite in the sedimentary cover of the Bitlis complex and in the Eocene Urse formation (after Oberhänsli *et al.* 2010).

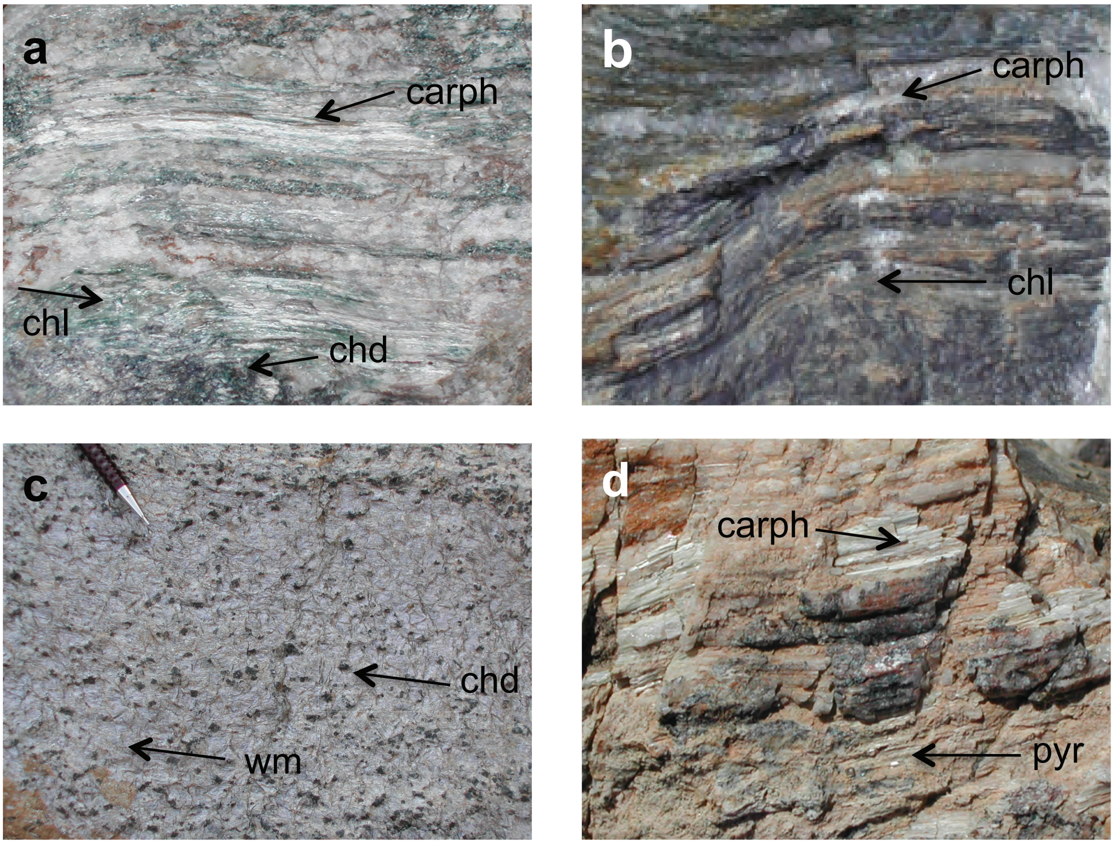

Figure 2. Rock samples showing HP minerals from the cover units of the Bitlis complex. **(a)** Carpholite-white mica fibres associated with quartz and chlorite, minute chloritoid along the quartz fibres (north of Çatak); **(b)** metapelite with chlorite and white mica; small quartz exudates contain relicts of carpholite (north of Çatak); **(c)** silvery chloritoid schist with white mica (Çatak); **(d)** carpholite and pyrophyllite layer in marble from the southern thrust-front of the Bitlis complex (south of Çatak, north of Narlı); wm– white mica; pyr– pyrophyllite; carph– Fe-Mg-carpholite; chl– chlorite; chd– chloritoid.

show mainly calcic amphiboles and sodic amphiboles are scarce.

In the metasedimentary cover of the Bitlis complex silvery metapelitic schists, intercalated with calcareous marbles, contain the assemblage chlorite-white mica-quartz. A greenschist metamorphic overprint is obvious at first glance. However, along the frontal (S) and basal parts of the sedimentary cover the assemblage Fe-Mg-carpholite-chlorite-white mica-quartz occurs. This is interpreted to represent the high-pressure peak event. In rare cases pyrophyllite-chlorite-Fe-Mg-carpholite assemblages testify prograde relicts. In internal parts of the complex most of the Fe-Mg-carpholite reacted to form chloritoid and only remained stable in quartz veins and nodules. The stable mineral assemblage is chloritoid-white mica-quartz-chlorite, sometimes associated with paragonite. A few samples contain kyanite and chloritoid; others chloritoid and epidote. In rare cases garnet, together with chloritoid, chlorite and white mica, is found. This indicates a low-pressure overprint after HP metamorphism. Mafic rocks associated with these metapelites contain sodic-calcic amphibole and rare glaucophane and testify to blueschist metamorphic conditions. The distribution of Fe-Mg-carpholite and glaucophane documents the extent of high-pressure low-temperature metamorphism all over the metasedimentary part of the Eastern Bitlis complex.

Representative compositions of metamorphic minerals of the Bitlis complex are compiled in Table 1. Electron microprobe analyses using natural and synthetic mineral standards at standard conditions (15 kV, 20 nA) were performed on Cameca SX 100 at GFZ Potsdam, at CAMPARIS Paris VI and on JEOL 5800 at Potsdam University.

Glaucophane in metabasites and Fe-Mg-carpholite in metapelites can be used to estimate the P-T conditions (e.g., Oberhänsli *et al.* 1995, 2001). Fe-Mg-carpholite has homogeneous compositions (X_{Mg}= 0.65–0.70 in marbles; X_{Mg}= 0.33–0.50 in metapelites). Chloritoid always has significantly lower X_{Mg} (0.05–0.35). Values of 8 are found for Fe-Mg partitioning coefficients of carpholite/chloritoid. This corresponds to values reported elsewhere for similar rock-types and PT conditions (Crete: Theye *et al.* 1992; Oman: Vidal & Theye 1996, Alps: Bousquet *et al.* 2002). Multiequilibrium calculations (Vidal *et al.* 1999; Vidal & Parra 2000; Parra *et al.* 2002; Rimmelé *et al.* 2005) using end members of chlorite (clinochlore, daphnite, sudoite, amesite) and white mica (celadonite, pyrophyllite, muscovite) produced P-T conditions indicating pressure at 0.8–1.0 GPa and temperature at 320°C for the prograde relicts (pyr-car), pressure at 1.0–1.1 GPa and temperature at 350–400°C for peak conditions (car-chl-wm) and temperature at 370–460°C at lower pressure at 0.3–0.6 GPa for the retrograde evolution (chd-chl-wm-ky) (Oberhänsli *et al.* 2010) (Figure 3). The Bitlis complex reveals a cold thermal evolution with a quasi-isothermal decompression.

Table 1. Representative electron microprobe analyses of HP-LT minerals from a metasediment sample of the Bitlis complex.

Van 36	chl		wm		chd		gt		car	
SiO_2	24.24	25.55	46.98	46.98	24.65	24.76	36.72	37.49	39.35	39.32
TiO_2	0.04	0.07	0.11	0.11	0.02	0.04	0.15	0.00	0.00	0.00
Al_2O_3	23.47	21.70	35.84	35.84	41.54	41.61	21.16	21.37	32.29	32.36
FeO	26.46	26.52	1.73	1.73	23.99	25.27	33.78	35.73	7.29	7.70
MnO	0.17	0.08	0.00	0.00	0.00	0.01	3.08	0.00	0.14	0.10
MgO	13.58	14.73	0.65	0.65	2.84	3.07	0.73	2.07	8.78	8.80
CaO	0.00	0.00	0.00	0.00	0.00	0.00	6.08	4.91	0.00	0.00
Na_2O	0.01	0.04	1.36	1.36	0.02	0.01	0.01	0.01	0.00	0.00
K_2O	0.01	0.00	9.26	9.26	0.00	0.02	0.02	0.00	0.00	0.00
F	0.02	0.17	0.00	0.00	0.00	0.00	0.00	0.00	2.45	1.80
Sum	87.99	88.85	95.93	95.93	93.06	94.77	101.74	101.58	90.30	90.07
cat p.f.u.	14	14	11	11	6	6	12	12	8	8
Si	2.56	2.67	3.09	3.09	2.02	1.99	2.95	2.98	2.03	2.02
Ti	0.00	0.01	0.01	0.01	0.00	0.00	0.01	0.00	0.00	0.00
Al	2.92	2.68	2.78	2.78	4.01	3.93	2.00	2.00	1.99	1.98
Fe	2.34	2.32	0.10	0.10	0.00	0.07	2.27	2.37	0.32	0.33
Mn	0.01	0.01	0.00	0.00	1.64	1.70	0.21	0.00	0.01	0.00
Mg	2.14	2.30	0.06	0.06	0.00	0.00	0.09	0.25	0.68	0.68
Ca	0.00	0.00	0.00	0.00	0.35	0.37	0.52	0.42	0.00	0.00
Na	0.00	0.01	0.17	0.17	0.00	0.00	0.00	0.00	0.00	0.00
K	0.00	0.00	0.78	0.78	0.00	0.00	0.00	0.00	0.00	0.00
F	0.02	0.11	0.00	0.00	0.00	0.00	0.00	0.00	0.41	0.29

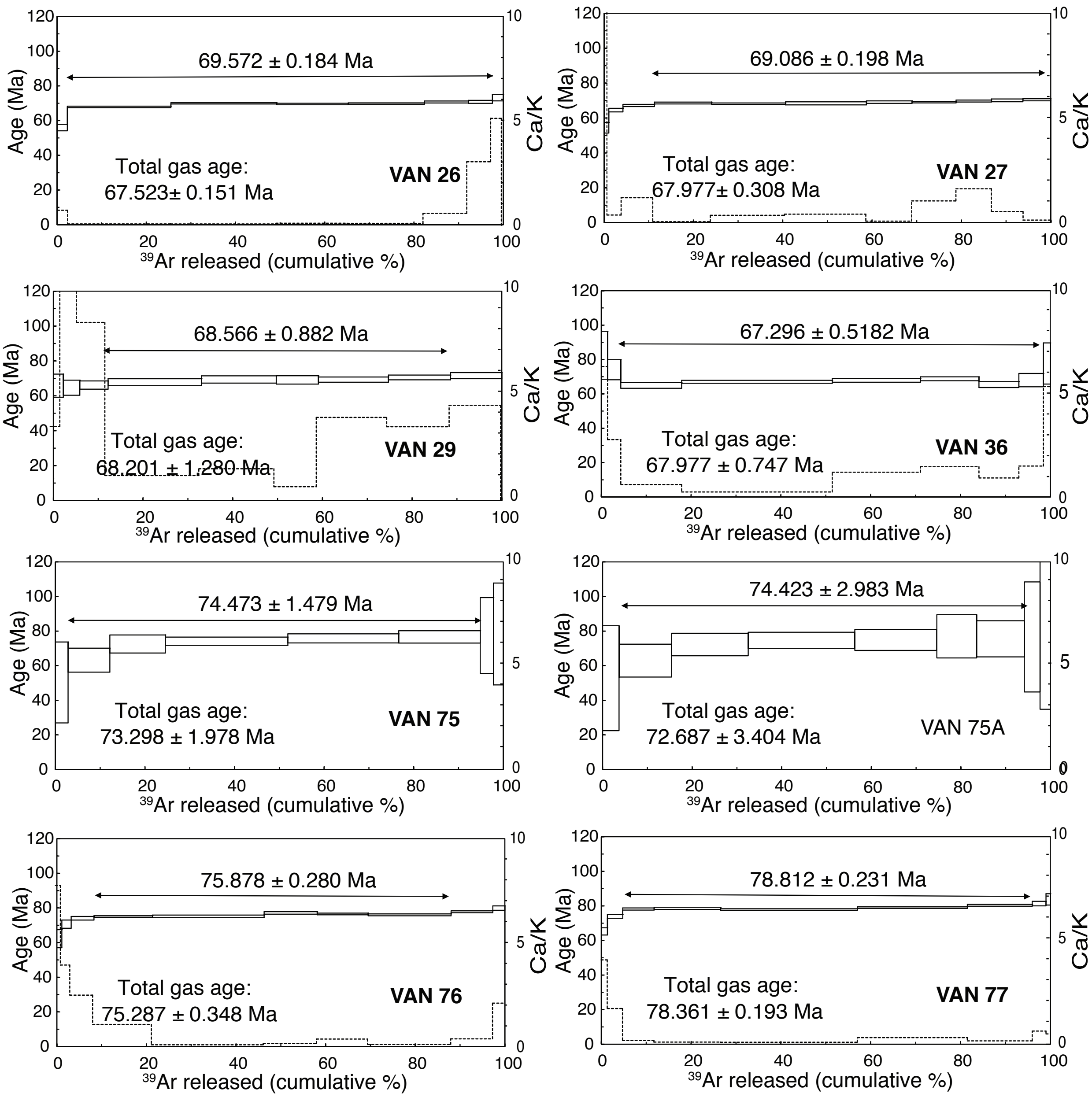

Figure 3. Ar plateau ages of white mica: mica of the assemblage carpholite-chlorite-white mica (samples: VAN 75, 75A, 76, 77) records the HP peak age, while mica of the assemblage chloritoid-chlorite-white mica-kyanite (VAN 26, 27, 29, 36) records the age of retrogression to greenschist facies.

Age of Metamorphism

Several white micas from carpholite-bearing metasediments (Figure 1a) were dated by laser $^{40}Ar/^{39}Ar$ method. These micas formed during peak metamorphism at temperatures below 400°C and might have recrystallized during exhumation and retrogression at temperatures below 460°C, still below the closing temperature of white mica (550–600°C, Villa 1998; Di Vincenzo *et al.* 2003) and therefore it is assumed that the ages can be related to the P-T conditions of the assemblage in which mica formed. White micas at peak and retrograde conditions have

Table 2. White mica $^{40}Ar/^{39}Ar$ dating results from HP metasediments from the Bitlis complex.

Van 26, white mica J = 0.001662

Laser output (W)	$^{40}Ar/^{39}Ar$	$^{37}Ar/^{39}Ar$	$^{36}Ar/^{39}Ar$	K/Ca	$^{40}Ar^*$	$^{39}Ar_K$	$^{40}Ar^*/^{39}Ar_K$	Age (±1s) Ma
0.014	38.19±0.35	0.41±2.97	65.27±1.50	1.44	49.63	2.31	18.96±0.63	55.97±1.86
0.018	24.60±0.11	0.04±0.26	5.16±0.08	14.46	93.82	23.21	23.08±0.11	67.89±0.42
0.020	24.04±0.07	0.04±0.28	0.88±0.04	14.77	98.94	23.71	23.78±0.08	69.94±0.36
0.022	24.01±0.07	0.06±0.63	1.22±0.13	9.98	98.53	16.03	23.66±0.12	69.57±0.43
0.024	23.98±0.07	0.06±0.48	0.82±0.12	10.63	99.01	17.08	23.74±0.10	69.81±0.40
0.026	24.33±0.10	0.32±0.96	1.11±0.22	1.81	98.83	9.86	24.06±0.17	70.73±0.57
t.f.	23.83±0.12	1.70±1.79	0.03±0.31	0.34	100.89	5.37	24.09±0.28	70.81±0.86

Plateau age: 69.6±0.2 Ma; total gas age: 67.5±0.2 Ma; Isocron age: 69.8±0.4 Ma

Van 27, white mica J = 0.001667

Laser output (W)	$^{40}Ar/^{39}Ar$	$^{37}Ar/^{39}Ar$	$^{36}Ar/^{39}Ar$	K/Ca	$^{40}Ar^*$	$^{39}Ar_K$	$^{40}Ar^*/^{39}Ar_K$	Age (±1s) Ma
0.014	42.33±0.72	8.18±6.25	85.16±1.43	0.07	43.06	1.06	18.37±1.04	54.42±3.03
0.016	23.99±0.07	0.25±2.34	7.37±0.44	2.38	91.05	3.16	21.85±0.34	64.53±1.02
0.018	23.90±0.13	0.73±1.03	4.21±0.20	0.81	95.19	7.05	22.76±0.19	67.19±0.62
0.020	23.88±0.14	0.06±0.50	2.16±0.10	9.62	97.37	12.82	23.25±0.16	68.59±0.53
0.022	23.75±0.10	0.24±0.30	2.29±0.07	2.46	97.28	16.54	23.11±0.11	68.20±0.42
0.024	23.67±0.08	0.27±0.30	1.80±0.93	2.16	97.91	18.11	23.18±0.29	68.40±0.88
t.f.	23.72±0.21	0.08±0.64	1.03±0.11	7.66	98.75	10.21	23.43±0.23	69.12±0.71

Plateau age: 69.1±0.2 Ma; total gas age: 68.0±0.3 Ma; Isocron age: 69.2±0.7 Ma

Van 29, white mica J = 0.00167

Laser output (W)	$^{40}Ar/^{39}Ar$	$^{37}Ar/^{39}Ar$	$^{36}Ar/^{39}Ar$	K/Ca	$^{40}Ar^*$	$^{39}Ar_K$	$^{40}Ar^*/^{39}Ar_K$	Age (±1s) Ma
0.012	1297.76±159	46.58±333.60	4208.87±523	0.01	4.63	0.09	62.90±61.52	180.20±167.73
0.014	82.82±1.12	2.04±14.14	206.03±4.64	0.29	26.81	2.13	22.25±2.28	65.81±6.64
0.016	31.19±0.87	9.86±9.27	36.64±1.27	0.06	69.40	3.67	21.85±1.49	64.65±4.32
0.018	26.34±0.47	4.87±4.80	15.93±0.84	0.12	84.54	6.31	22.37±0.81	66.18±2.36
0.020	24.59±0.64	0.70±1.83	5.93±0.54	0.84	93.24	20.84	22.94±0.68	67.82±1.99
0.022	24.57±0.67	0.88±1.94	4.16±0.37	0.67	95.46	16.66	23.48±0.71	69.39±2.09
t.f.	24.85±0.58	0.39±3.83	5.15±1.08	1.50	94.08	9.40	23.39±0.82	69.13±2.39

Plateau age: 68.6±0.9 Ma; total gas age: 68.2±1.3 Ma; Isocron age: 68.8±2.2 Ma

Table 2. (Contunied).

Van 36, white mica J = 0.001670

Laser output (W)	$^{40}Ar/^{39}Ar$	$^{37}Ar/^{39}Ar$	$^{36}Ar/^{39}Ar$	K/Ca	$^{40}Ar^*$	$^{39}Ar_K$	$^{40}Ar^*/^{39}Ar_K$	Age (±1s) Ma
0.012	539.17±41.90	35.36±283.69	1732.57±142	0.02	5.90	0.13	32.91±43.51	96.53±124.27
0.014	83.43±1.99	3.72±29.39	189.58±9.25	0.16	33.44	1.27	28.00±4.84	82.44±13.93
0.016	40.23±0.60	1.64±13.49	52.08±2.79	0.36	62.28	2.94	25.09±2.02	74.06±5.85
0.018	23.34±0.40	0.36±2.79	4.94±0.60	1.65	93.94	13.56	21.94±0.56	64.91±1.66
0.020	23.34±0.23	0.14±1.07	2.37±0.29	4.08	97.08	33.54	22.66±0.28	67.02±0.86
0.022	23.40±0.27	0.71±1.74	1.86±0.41	0.83	98.04	19.65	22.96±0.37	67.88±1.11
t.f.	24.03±0.19	0.87±1.94	3.03±0.72	0.68	96.75	13.03	23.27±0.38	68.78±1.14

Plateau age: 67.3±0.5 Ma; total gas age: 67.7±0.7 Ma; Isocron age: 68.0±0.7 Ma

Van 75, white mica J = 0.00177

Laser output (W)	$^{40}Ar/^{39}Ar$	$^{37}Ar/^{39}Ar$	$^{36}Ar/^{39}Ar$	K/Ca	$^{40}Ar^*$	$^{39}Ar_K$	$^{40}Ar^*/^{39}Ar_K$	Age (±1s) Ma
0.012	139.06±6.27	2.74±2740.20	448.76±28.29	0.21	4.89	0.06	6.82±356.18	21.59±1120.66
0.014	24.12±0.22	0.06±57.91	27.43±0.72	10.16	66.43	2.77	16.02±7.55	50.32±23.39
0.016	21.72±0.03	0.02±17.22	5.15±0.11	34.16	93.00	9.33	20.20±2.25	63.21±6.93
0.018	24.44±0.05	0.01±12.98	4.03±0.10	45.33	95.13	12.39	23.25±1.70	72.55±5.22
0.020	24.56±0.05	0.01±5.88	2.67±0.04	99.98	96.79	27.35	23.77±0.77	74.15±2.38
0.022	25.00±0.04	0.01±6.50	2.35±0.05	90.49	97.22	24.76	24.31±0.86	75.79±2.63
0.024	25.74±0.03	0.01±8.85	3.90±0.09	66.45	95.53	18.19	24.59±1.16	76.65±3.57
0.026	26.90±0.16	0.05±54.66	6.98±0.48	10.76	92.36	2.95	24.85±7.19	77.44±21.93
t.f.	41.63±0.24	0.07±73.35	55.82±1.24	8.02	60.40	2.20	25.14±9.66	78.34±29.44

Plateau age: 74.5±1.5 Ma; total gas age: 73.3±2 Ma; Isocron age: 73.8±7.7 Ma

Van 75A, white mica J = 0.00177

Laser output (W)	$^{40}Ar/^{39}Ar$	$^{37}Ar/^{39}Ar$	$^{36}Ar/^{39}Ar$	K/Ca	$^{40}Ar^*$	$^{39}Ar_K$	$^{40}Ar^*/^{39}Ar_K$	Age (±1s) Ma
0.014	71.59±0.37	0.08±75.13	185.37±1.59	7.83	23.50	3.68	16.82±9.81	52.79±30.33
0.016	36.83±0.10	0.02±23.58	56.58±0.56	24.95	54.61	11.73	20.11±3.09	62.94±9.50
0.018	28.25±0.08	0.02±16.16	17.27±0.18	36.40	81.94	17.12	23.15±2.12	72.24±6.50
0.020	25.96±0.16	0.01±11.52	6.83±0.13	51.07	92.23	23.80	23.95±1.52	74.68±4.65
0.022	25.57±0.08	0.02±15.13	5.26±0.10	38.88	93.92	18.31	24.02±1.99	74.91±6.08
0.024	26.24±0.09	0.03±31.19	5.20±0.20	18.86	94.16	8.89	24.71±4.10	77.01±12.52
0.026	25.68±0.05	0.03±26.03	4.92±0.14	22.60	94.35	10.66	24.23±3.42	75.54±10.45
0.028	27.74±0.22	0.08±79.27	10.71±0.53	7.42	88.63	3.50	24.58±10.42	76.63±31.81
t.f.	59.40±0.33	0.12±119.66	111.03±1.97	4.92	44.79	2.32	26.61±15.78	82.81±48.00

Plateau age: 74.4±2.8 Ma; total gas age: 72.7±3.4 Ma; Isocron age: 73.8±7.7 Ma

Table 2. (Contunied).

Van 76, white mica J = 0.001684

Laser output (W)	$^{40}Ar/^{39}Ar$	$^{37}Ar/^{39}Ar$	$^{36}Ar/^{39}Ar$	K/Ca	$^{40}Ar^*$	$^{39}Ar_K$	$^{40}Ar^*/^{39}Ar_K$	Age (±1s) Ma
0.014	163.84±1.741141542	4.55±2.82	486.18±6.516432247	0.13	12.67	1.11	20.85±1.77	62.27±5.21
0.016	30.19±0.745949265	2.29±2.36	23.08±1.146385174	0.26	78.40	2.09	23.72±0.81	70.66±2.37
0.018	27.07±0.31064942	1.44±0.72	8.15±0.476631696	0.41	91.80	5.09	24.88±0.34	74.06±1.04
0.02	26.66±0.097728773	0.61±0.41	5.14±0.159107786	0.97	94.60	13.07	25.23±0.12	75.08±0.45
0.022	25.99±0.229732194	0.03±0.21	2.47±0.127502305	19.15	97.20	24.91	25.26±0.23	75.16±0.74
0.024	26.41±0.21531416	0.06±0.42	1.61±0.1487715	9.11	98.23	11.85	25.94±0.23	77.14±0.72
t.f.	26.15±0.08451482	0.19±0.63	1.50±0.199932551	3.04	98.40	11.37	25.73±0.13	76.54±0.49

Plateau age: 75.9±0.3 Ma; total gas age: 75.3±0.3 Ma; Isocron age: 76.0±0.7 Ma

Van 77, white mica J = 0.001681

Laser output (W)	$^{40}Ar/^{39}Ar$	$^{37}Ar/^{39}Ar$	$^{36}Ar/^{39}Ar$	K/Ca	$^{40}Ar^*$	$^{39}Ar_K$	$^{40}Ar^*/^{39}Ar_K$	Age (±1s) Ma
0.014	78.28±0.44	2.38±1.31	191.98±2.29	0.25	27.93	1.36	21.91±0.71	65.26±2.09
0.016	29.16±0.34	1.00±0.70	15.03±0.54	0.59	85.22	3.41	24.87±0.36	73.90±1.10
0.018	27.38±0.12	0.09±0.86	3.52±0.29	6.79	96.24	6.99	26.35±0.19	78.20±0.62
0.020	26.91±0.17	0.04±0.43	1.49±0.14	14.40	98.38	14.82	26.48±0.19	78.57±0.62
0.022	26.60±0.11	0.04±0.30	1.19±0.07	16.46	98.69	30.46	26.25±0.12	77.91±0.45
0.024	26.96±0.10	0.17±0.29	1.20±0.10	3.49	98.76	24.48	26.63±0.11	79.01±0.45
t.f.	27.43±0.12	0.08±0.57	1.16±0.12	7.80	98.78	14.45	27.09±0.14	80.35±0.52

Plateau age: 78.8±0.2 Ma; total gas age: 78.4±0.2 Ma; Isocron age: 78.8±0.6 Ma

similar compositions, are not related to breakdown reactions of carpholite, but rather represent products of continuous recrystallization during heating.

Samples were analysed at the argon geochronology laboratory of the Institute of Earth and Environmental Sciences, University of Potsdam (Germany) and irradiated for 96 hours at the FRG-1 facility of the GKSS research centre at Geesthacht (Germany). The neutron flux variation over the length of the sample capsule was monitored by Fish Canyon Tuff Sanidine and calculated using a linear fit. Interference correction factors were obtained by analysing CaF_2 and K_2SO_4 irradiated together with the samples. Mean blank values during the experiments for ^{40}Ar, ^{39}Ar, ^{37}Ar, and ^{36}Ar were $1.46e^{-4}$, $7.32e^{-8}$, $8.95e^{-9}$, $4.35e^{-6}$ respectively. Age spectra were produced from 3 respectively 7 grains and data corrected for blank, mass discrimination, ^{37}Ar and ^{39}Ar decay. They have been fitted on $^{36}Ar/^{40}Ar$ vs $^{39}Ar/^{40}Ar$ isochron plots (York 1969). Results are presented in Table 2 and Figure 3.

Excess argon may hamper the interpretation of $^{40}Ar/^{39}Ar$ white mica ages subjected to very high-pressure conditions (e.g., Li *et al.* 1994; Arnaud & Kelly 1995; Ruffet *et al.* 1995). Strongly deformed, K-poor bulk compositions at low high-pressure conditions close to closure temperatures (550–600 °C, Villa 1998) are barely suitable to incorporate excess argon in white mica (Oberhänsli *et al.* 1998; Sherlok & Kelley 2002).

Two samples from Gevaş, on the northern contact of the Bitlis complex (VAN 75, 75A; Figure 1a) yield concordant apparent ages, which define plateau ages of 74.5±1.5 Ma, and 74.4±3.0 Ma, respectively. Isochron ages are similar to the plateau ages with intercept ages of 73.8±7.8 Ma and 73.8±7.7 Ma, respectively. Two samples from areas south and north of Gevaş (VAN 76, 77; Figure 1a) yield similar plateau ages of 75.9±0.3 Ma and 78.8±0.2 Ma while four samples along the Çatak valley (VAN 26, 27, 29, 36; Figure 1a) yield from north to south 69.6±0.2 Ma, 69.1±0.2 Ma, 68.6±0.9 Ma and 67.3±0.6 Ma (Figure 3). The corresponding isochron ages are: 76.0±0.7 Ma, 78.8±0.6 Ma and 69.8±0.4 Ma, 69.2±0.7 Ma, 68.8±2.2 Ma, 68.0±0.7 Ma. The age analyses cluster in two groups at 74–79 Ma and 67–70 Ma. On one hand, these age groups correlate with regional distribution and on the other they clearly reflect the P-T evolution of the mineral assemblages (Figures 1a & 4). Regionally the older ages stem from the northern (higher?) part of the complex while the younger ages were found along the basal and towards the frontal parts of the easternmost Bitlis complex. Different relict mineral assemblages representing the HP events are variously well preserved at different tectonic levels. Among the mineral assemblages, the first, slightly older group stems from carpholite-chlorite-white mica-bearing rocks, while the second group, younger by 5 to 10 Ma, was dated using white mica from chloritoid-chlorite±kyanite assemblages with relict carpholite.

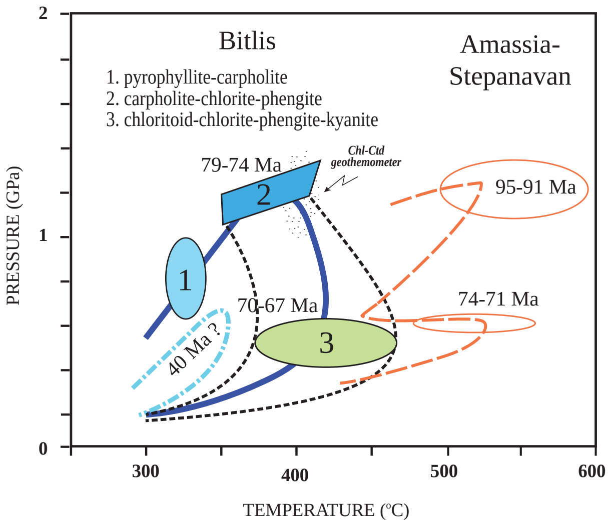

Figure 4. Pressure-temperature diagram compiling the data for the Bitlis metapelites (after Oberhänsli *et al.* 2010). 1– Prograde assemblages with pyrophyllite relicts; 2– Peak assemblages with carpholite and carpholite-chloritoid; 3– retrograde assemblages with chloritoid, chlorite, garnet and kyanite. The inferred retrograde paths (dots) range from isothermal decompression to moderate heating during decompression. PT path (dash-dot) and estimated age (Oberhänsli *et al.* 2010) for the Eocene blueschists of the Urse Formation are somewhat speculative. For comparison the P-T data, ages and the inferred PT path from Rolland *et al.* (2008) are given. Differences in PT paths as well as the time span for the transition from HP to LP are evident (see text).

Discussion

Mineral assemblages in the cover sequence of the eastern Bitlis complex record subduction-related

HP-LT metamorphism. The studied pyrophyllite-bearing assemblages record a prograde evolution, and low temperatures at elevated pressures (Figure 4-1). Samples with carpholite and carpholite relicts record higher temperatures at high pressures (Figure 4-2). Chloritoid-bearing samples with carpholite relicts in quartz indicate similar conditions. Chloritoid samples lacking carpholite relicts (Figure 4-3) indicate a wider range of temperatures at lower pressures. Since kyanite remained stable together with chloritoid temperatures cannot have exceeded 480°C at 0.5 GPa because the reaction chloritoid + kyanite <-> chlorite + staurolite (Spear & Cheney 1989) was never overstepped. Garnet and epidote indicate decompression (Bousquet *et al.* 2008). Therefore isothermal decompression or decompression at slightly elevated temperatures is inferred for the retrogression from HP-LT. Temperatures recorded in metamorphic rocks of the Bitlis complex never exceeded 460°C during the Mesozoic and Cenozoic evolution (Oberhänsli *et al.* 2010), thus indicating cold almost isothermal decompression. This fits well with observations from Tethyan metasediments in Western Turkey, in the Lycian Nappes (Rimmelé *et al.* 2002), and Afyon Zone (Candan *et al.* 2005).

However, these P-T conditions contrast with those determined for the Amassia-Stepanavan Suture Zone (Figure 4) to the north, in Armenia (Rolland *et al.* 2008). There, based on glaucophane-crossite, aegirine and the absence of lawsonite, HP conditions at pressures of 1.2±0.15 GPa and temperatures of 545±64°C and, for the LP-MT parageneses (garnet-chlorite-pargasite-albite-clinozoisite), pressures of 0.57±0.02 GPa and temperatures of 505±67°C were estimated. Metamorphism and exhumation occurred at higher temperatures than those recorded in the Bitlis complex. Subduction-related metamorphism, as well as the later LP-MT phases, point to a relatively hot subduction-type geotherm of 10–15°C/km (Rolland *et al*. 2008). This is slightly higher than that observed in the Bitlis complex (≤ 10°C/km).

The time interval between the HP event (Figure 4-2) and the greenschist event (Figure 4-3) is short and supports our interpretation of a simple uniform PT-path. This contrasts with the northern suture zone in Armenia, where a time gap of ca. 20 Ma is recorded between the HP and the LP-MT event (Figure 4) and a two-phase exhumation history has been suggested (Rolland *et al.* 2008).

The late Cretaceous age of the blueschist metamorphism in the Bitlis complex is compatible with geological constraints as well as observations from the lesser Caucasus, where HP metamorphism is dated at 95–90 Ma (Rolland *et al.* 2008). It is slightly younger than the HP metamorphism of the Tavşanlı zone in western Anatolia (ca. 80 Ma, e.g., Okay & Kelley 1994; Sherlok *et al.* 1999) but fits the age of metamorphism (K/Ar: 71.2±3.6 Ma, Hempton 1985) from the Pütürge massif. Interestingly, in the Amassia-Stepanavan area blueschist metamorphism (95–90 Ma) was followed by a much younger greenschist facies event, dated at 74–71 Ma (Rolland *et al.* 2008), leaving a rather long time span of ca. 20 Ma for exhumation. The Bitlis samples, however, clearly reveal rapid exhumation within 5–10 Ma.

The overturned northern contact of the Bitlis complex near Gevaş was considered to be the metamorphic sole of an obducted ophiolite (Yılmaz *et al.* 1981). However the 'ophiolite' is more like an ophiolitic mélange, as shown by its blocky nature, the compositions of blocks and matrix and its lack of metamorphism, and is comparable to the Yüksekova complex. HP-LT metamorphic conditions (1.2 GPa; ≤ 460°C), demonstrated in the Bitlis complex but not in the ophiolitic mélange near Gevaş, thus exclude obduction and metamorphic sole. The non-metamorphic ophiolitic mélanges of the Yüksekova complex derived from the oceanic realm between the Anatolide-Tauride (South Armenian?) and Bitlis blocks. They were thrust over the exhuming Bitlis complex. After collision with the Arabian plate, which started in the Oligo–Miocene (ca. 20 Ma; Okay *et al.* 2010), back-thrusting emplaced the northern part of the Bitlis complex locally over the Yüksekova complex in Gevaş.

From the petrography it is obvious that the Bitlis complex and some Eocene formations experienced a subduction event and remained cold during their later geodynamic evolution. These facts were not considered in geodynamic evolution schemes published earlier (Yılmaz 1993; Şengör *et al.* 2003; Keskin 2003), in which the scenarios did not focus on the metamorphic evolution of the Bitlis complex.

South of the Bitlis complex, based on the evolution of Tertiary sediments, Yılmaz (1993) assumed an intra-oceanic subduction between a northern block (Bitlis) and the Arabian plate during the Late Maastrichtian to Early Eocene. This model accounts for Eocene to Oligocene subduction south of the Bitlis complex, as recently confirmed by blueschist findings (Oberhänsli *et al.* 2010), without detailing the metamorphic evolution either in the Bitlis complex or in the underlying Tertiary nappes. Timing of the sedimentary evolution south of the Bitlis complex is well constrained in this model. However, the geodynamics of nappe stacking of the 'metamorphic massifs' since the Late Maastrichtian is little constrained. Yılmaz's (1993) compilation leaves only a short time span for the exhumation of the Eocene blueschists, since they should be exhumed by the Early Miocene. This fits well with apatite fission track data, recording the onset of exhumation by ca. 20 Ma (Okay *et al.* 2010).

Other models focus on the geodynamic evolution north of the Bitlis complex (e.g., Şengör *et al.* 2003; Keskin 2003). Although both models focus on the Tertiary evolution of the area they start with a late Cretaceous to Palaeocene settings, assuming Bitlis was in the upper plate at the surface. Our data, however, clearly show that subduction processes continued throughout the Campanian to the end of the Maastrichtian, leaving too little time for the development of oceanic basins as assumed in these reconstructions.

The metamorphic evolution and especially the regional preservation of HP-LT assemblages in the sedimentary cover call for an adapted geodynamic scenario. At present the Bitlis complex is moving northwards below a mélange equivalent to the Yüksekova complex partly buried under the Quaternary volcanic cover, or eventually the Anatolide-Tauride Block. Its frontal parts are thrust southward over Cenozoic complexes and the Arabian platform. Investigations of the Sevan ophiolite in Armenia (Sosson *et al.* 2010) and HP assemblages along the Amassia-Stepanavan ophiolitic suture (Rolland *et al.* 2008) as well as its correlation with the İzmir-Ankara-Erzincan suture and the ages for the Bitlis HP evolution infer that the Bitlis block underwent subduction under the amalgamated Eurasian Tauride plate during the latest Cretaceous. As suggested in the MEBE palinspastic maps, the Bitlis block might have separated from the Taurus platform during Aptian to Cenomanian times (Barrier & Vrielynck 2008; see also Şengör & Yılmaz 1981). These maps were compiled taking the Bitlis HP into account and are some of the possibilities to create an oceanic basin north of the Bitlis block. Other models prefer to associate the Bitlis block with the Arabian platform (Dercourt *et al.* 1992) and to separate it from the Arabian platform as the Bitlis/Bistun block. To some extent this is also supported by the finding of rudist-bearing limestone blocks which were derived from Arabian platform in the Gevaş melange (Özer 1992).

Two hypotheses for the geodynamic evolution can be put forward: (i) subduction of the Bitlis block below the Anatolide-Tauride platform or (ii) subduction below oceanic crust or the East Anatolian Accretionary Complex respectively. Neither of them can be tested due to extensive Miocene basins and Quaternary volcanic cover to the north of the Bitlis complex.

The first case, discussed in the previous paragraph, allows for shallow subduction of continental material (basement and cover). In this case the Cretaceous mélanges of the Yüksekova unit overlying the imbricated Tertiary units must be derived laterally from the East. They could possibly be related to the Khoy ophiolite (Iran). This fits with the coincidence of the western limit of the Yüksekova units with the eastern limits of the Bitlis complex.

The second hypothesis envisages the Yüksekova mélange as part of an East Anatolian Accretionary Complex. Subduction of an extensively stretched continental margin (Galicia type) below oceanic crust would be possible. The coherence and thickness of the continental crust of the Bitlis complex, where the typical association of continental crust and mantle rocks, as well as indications that rift-related LP-HT metamorphism is missing, do not support this hypothesis.

We have adapted the first hypothesis for our reconstruction (Figure 5).

After northward subduction and blueschist metamorphism (74–79 Ma), the Bitlis complex

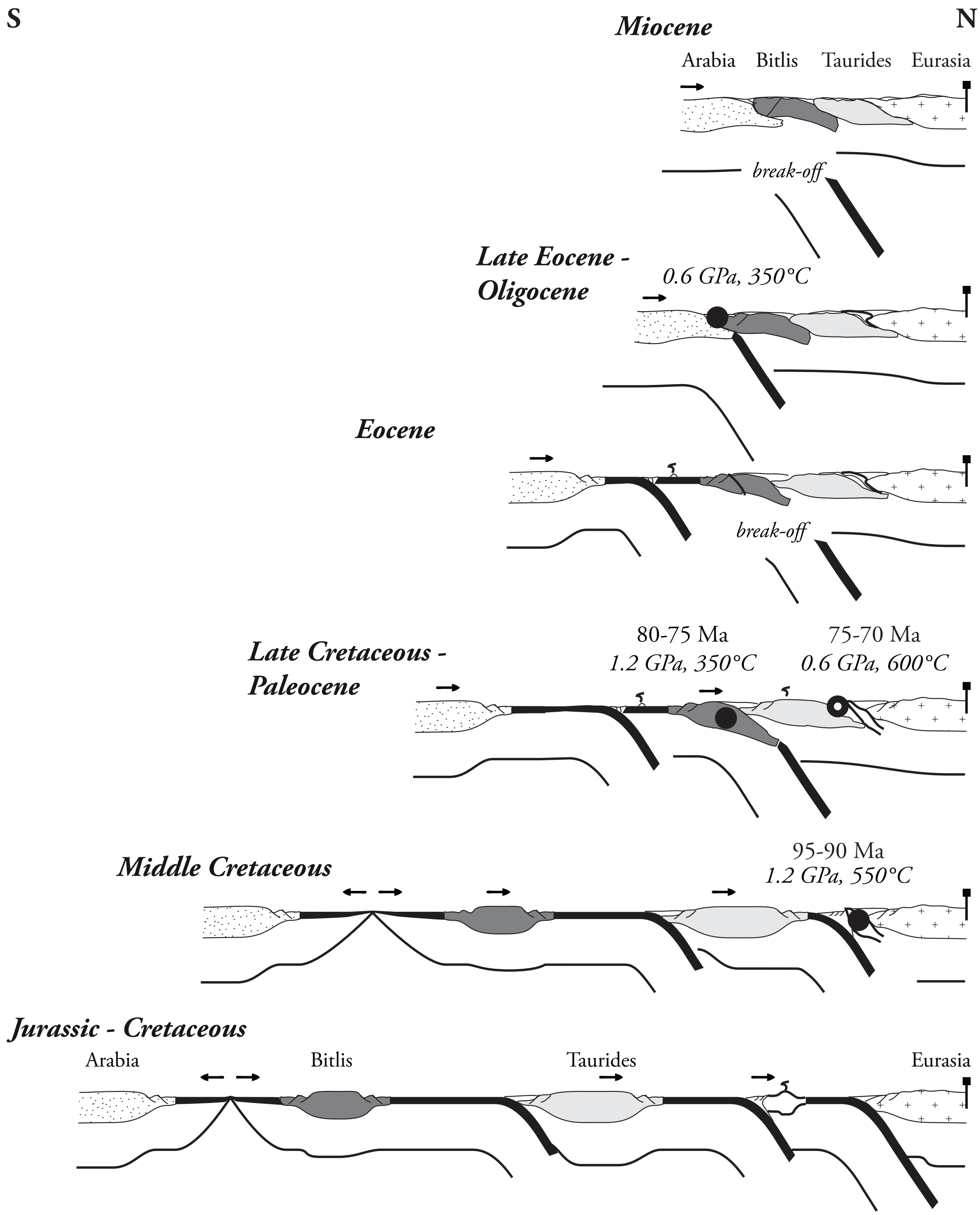

Figure 5. Schematic geodynamic cross-sections. A southward migration of subduction is inferred from the ages of HP metamorphism and from the sedimentary record (e.g., Yılmaz 1993). For the Anatolide-Tauride block only Taurides is used. Black dots– pressure-dominated metamorphism; black and white dots– temperature-dominated metamorphism.

was exhumed rapidly during the latest Cretaceous (67–70 Ma). This is further supported by the Bitlis metamorphic units in the frontal part being imbricated with non-metamorphic, fresh and well-preserved Middle Eocene pillow lava of the Maden complex (sensu Perinçek & Özkaya 1981). The blueschist metamorphism in the Palaeocene–Eocene rocks of the Urse formation (Maden complex sensu Rigo de Righi & Cortesini 1964; Yiğitbaş & Yılmaz 1996) probably occurred during Late Eocene–Early Oligocene, since exhumation was completed by late Oligocene to Miocene times (Yılmaz 1993; Oberhänsli *et al.* 2010). This is also supported by apatite fission track data from Eocene sandstones in the same areas (Okay *et al*. 2010). Thus a time gap of ca. 20 Ma after the exhumation of HP rocks to LP-MT conditions in the Bitlis complex and exhumation of the Tertiary HP exists. While subduction of oceanic crust north of the Arabian margin has continued since the Late Cretaceous, continental collision of Arabia with the amalgamated Tauride block (Bitlis complex, Tauride block, South Armenian block etc.) started during the Miocene (Okay *et al.* 2010). A simple P-T path is recorded in the Bitlis complex because stacking of continental crust occurred only after exhumation of the HP complexes.

Studies of carpholite-bearing blueschists in the Alps showed a systematic influence of crustal stacking and related heating after the HP evolution, leading to bimodal exhumation paths (Wiederkehr *et al.* 2008). Similar bimodal P-T paths are recorded from the Amassia-Stepanavan suture in Armenia (Rolland *et al*. 2008) where, following subduction, immediate continental collision of the Anatolide-Tauride Block with Eurasia occurred. This stacking of continental material below the HP units, delayed by ca. 20 Ma, adds mechanical as well as thermal energy to the system. Thus deformation patterns and metamorphic evolution of the LP-MT event are distinct from the HP-LT event.

Conclusion

The eastern Bitlis complex exhibits subduction-related HP-LT metamorphic conditions. The PT evolution was reconstructed with three typical mineral assemblages recording prograde (0.8–1.0 GPa; 320°C), peak (1.0–1.1 GPa; 350–400°C) and retrograde (0.3–0.6 GPa; 370–460°C) conditions. While the prograde assemblage contains pyrophyllite not suitable for Ar dating, the peak and retrograde assemblages contain white mica. The peak assemblages consistently gave 74–79 Ma while the retrograde assemblages cluster around 67–70 Ma. These age data, combined with the petrological information, depict a simple clockwise cold HP path with almost isothermal decompression and rapid exhumation. This contrasts with the conditions recorded along the Amassia-Stepanavan suture, where a considerably warmer bimodal PT path was recorded. The difference in P-T-t evolution is interpreted as caused by subduction, followed by continental collision after 20 Ma in the Amassia-Stepanavan suture, in contrast to the Bitlis complex, where exhumation occurred rapidly after 5 to 10 Ma. Meanwhile, to the south oceanic subduction was still continuing, having started before deposition of the Miocene basins, thus ca. 40 Ma before the onset of collision of the Arabian continental crust. To account for the HP evolution in the Bitlis complex and the Eocene sediments south of it, a geodynamic scenario with southward stepping subduction zones is envisaged.

Acknowledgements

We thank the MEBE team in Paris, Marie Françoise Brunet, Eric Barrier and Jean Paul Cadet for their support. We also enjoyed discussion and fieldwork with Marc Sosson, Yan Rolland and Ghazar Galoyan. R.O. and A.I.O. express their thanks to Muharrem Satır for having shared his scientific life with them on several occasions. An anonymous reviewer is warmly acknowledged for having made us think in more detail about the Bitlis complex.

References

Arnaud, N.O. & Kelly, S. 1995. Evidence for excess Ar during high-pressure metamorphism in the Dora Maira massif (western Alps, Italy) using an ultra-violet laser ablation microprobe $^{40}Ar/^{39}Ar$ technique. *Contributions to Mineralogy and Petrology* **121**, 1–11.

Barrier, E. & Vrielynck, B. 2008. *Plate Tectonic Maps of the Middle East.* MEBE Program, CGMW, Paris.

Boray, A. 1975. Bitlis dolayının yapısı ve metamorfizması [The structure and metamorphism of the Bitlis area] *Türkiye Jeoloji Kurultayı Bülteni* 18, 81–84 [in Turkish with English abstract].

Bousquet, R., Goffé, B., Vidal, O., Oberhänsli, R. & Patriat, M. 2002. The tectono-metamorphic history of the Valaisan domain from the Western to the Central Alps: new constraints on the evolution of the Alps. *Bulletin of the Geological Society of America* **114**, 207–225.

Bousquet, R., Oberhänsli, R., Goffé, B., Wiederkehr, M., Koller, F. Schmid, S., Schuster, R., Engi, M., Berger, A. & Martinotti, G. 2008. Metamorphism of metasediments at the scale of an orogen: a key to the Tertiary geodynamic evolution of the Alps. *In*: Fügenschuh, S. & Froitzheim, N. (eds), *Tectonic Aspects of the Alpine-Dinaride-Carpathian System*. Geological Society, London, Special Publications **298**, 393–411.

Candan, O., Çetinkaplan, M., Oberhänsli, R., Rimmelé, G. & Akal, C. 2005. Alpine high-P/low-T metamorphism of the Afyon Zone and implications for the metamorphic evolution of Western Anatolia. *Lithos* **84**, 102–124.

Çağlayan, M.A., Önal, R.N., Şengün, M. & Yurtsever, A. 1984. Structural setting of the Bitlis Massif. *In*: Tekeli, O. & Göncüoğlu, M.C. (eds), *Geology of the Taurus Belt*. Proceedings of the International Symposium on the Geology of the Taurus Belt, Ankara, 245–254.

Çolakoğlu, A. 2009. Geology and geochemical characteristics of Gevas listwaenites (Van, Turkey). *Journal of the Earth Sciences Application and Research Centre of Hacettepe University* **30**, 59–81.

Dercourt, J. Ricou, L. & Vrielynk, B. 1992. *Atlas Tethys Palaeoenvironmental Maps*. CGMW, Paris.

Di Vincenzo, G., Carosi, R. & Palmeri, R. 2003. The relationship between tectono-metamorphic evolution and argon isotope records in white mica: constraints from in situ ^{40}Ar-^{39}Ar laser analysis of the Variscan basement of Sardinia (Italy). *Journal of Petrology* **45**, 1013–1043.

Gök, R., Pasyanos, M.E. & Zor, E. 2007. Lithospheric structure of the continent–continent collision zone: eastern Turkey. *Geophysical Journal International* **169**, 1079–1088.

Göncüoğlu, M.C. & Turhan, N. 1984. Geology of the Bitlis metamorphic belt. *In*: Tekeli, O. & Göncüoğlu, M.C. (eds), *Geology of the Taurus Belt*. Proceedings of the International Symposium on the Geology of the Taurus Belt, Ankara, 237–244.

Göncüoğlu, M.C. & Turhan, N. 1992. *Muş-I33 Sheet: 100 000 Scale Geological Map Series of Turkey*. Maden Tetkik ve Arama Genel Müdürlüğü, Ankara.

Göncüoğlu, M.C. & Turhan, N. 1997. Rock units and metamorphism of the basement and Lower Paleozoic cover of the Bitlis Metamorphic Complex, SE Turkey. *In*: Göncüoğlu, M.C. & Derman, A.S. (eds), *Lower Paleozoic Evolution in Northwest Gondwana*. Turkish Association of Petroleum Geology, Special Publications **3**, 75–81.

Hall, R. 1976. Ophiolite emplacement and the evolution of the Taurus suture zone, southeastern Turkey. *Bulletin of the Geological Society of America* **87**, 1078–1088.

Helvaci, C. & Griffin, W.L. 1984. Rb-Sr geochronology of the Bitlis Massif, Avnik (Bingöl) area, S.E. Turkey. *In*: Dixon, J.E. & Robertson, A.H.F. (eds), *The Geological Evolution of the Eastern Mediterranean*. Geological Society, London, Special Publications **17**, 403–413.

Hempton, M.R. 1985. Structure and deformation history of the Bitlis suture near Lake Hazar, southeastern Turkey. *Bulletin of the Geological Society of America* **96**, 233–243.

Horstink, J. 1971 The Late Cretaceous and Tertiary geological evolution of eastern Turkey. *Proceedings, 1. Petrol Kongresi*, 25–41 [in Turkish with English abstract].

Kellogg, H.E. 1960. *Stratigraphic Report, Hazro Area, Petroleum District V. SE Turkey*. Unpublished Report, Ankara.

Keskin, M. 2003. Magma generation by slab steepening and breakoff beneath a subduction-accretion complex: an alternative model for collision-related volcanism in Eastern Anatolia, Turkey. *Geophysical Research Letters* **30**, 1–4.

Li, S., Wang, S., Chen, Y., Liu, D., Qiu, J., Zhou, H. & Zhang, Z. 1994. Excess argon in phengites from eclogite: evidence from dating of eclogite minerals by Sm-Nd, Rb-Sr, ^{40}Ar/^{39}Ar methods. *Chemical Geology* **112**, 343–350.

Oberhänsli, R., Goffé, B. & Bousquet, R. 1995. Record of a HP-LT metamorphic evolution in the Valais zone: geodynamic implications. *Bolletino del Museo Regionale delle Scienze naturali Torino* **13**, 221–240.

Oberhänsli, R., Monié, P., Candan, O., Warkus, F.C., Partsch, J.H. & Dora, O.Ö. 1998. The age of blueschist metamorphism in the Mesozoic cover series of the Menderes Massif. *Schweizerische Mineralogische und Petrographische Mitteilungen* **78**, 309–316.

Oberhänsli, R., Partsch, J., Candan, O. & Çetinkaplan, M. 2001. First occurrence of Fe-Mg-carpholite documenting a high pressure metamorphism in the metasediments of the Lycian Nappes, SW Turkey. *International Journal of Earth Sciences* **89**, 867–873.

Oberhänsli, R., Candan, O., Bousquet, R., Rimmele, G., Okay, A.I. & Goff, J. 2010. Alpine HP Evolution of the eastern Bitlis complex, SE Turkey. *In*: Sosson M., Kaymakci, N., Stephenson, R., Strarostenko, V. & Bergerat, F. (eds), *Sedimentary Basins, Tectonics from Black Sea an Caucasus to the Arabian Platform*. Geological Society, London, Special Publications **340**, 461–483.

Okay, A.I., Arman, M.B. & Göncüoğlu, M.C. 1985. Petrology and phase relations of the kyanite-eclogites from Eastern Turkey. *Contributions to Mineralogy and Petrology* **91**, 196–204.

Okay, A.I. & Kelley, S.P. 1994. Jadeite and chloritoid schists from northwest Turkey: tectonic setting, petrology and geochronology. *Journal of Metamorphic Geology* **12**, 155–166.

Okay, A.I., Zattin, M. & Cavazza, W. 2010. Apatite fission-track data for the Miocene Arabia-Eurasia collision. *Geology* **38**, 35–38.

Özer, S. 1992. Presence of rudist-bearing limestone blocks derived from the Arabian Platform in Gevaş (Van) ophiolite. *Maden Tektik ve Arama Bulletin* **114**, 75–82 [in Turkish with English abstract].

Özer, S. 2005. Two new species of canaliculate rudists (Dictyoptychidae) from southeastern Turkey. *Geobios-Lyon* **38**, 235–245.

Parra, T. Vidal, O. & Jolivet, L. 2002. Relation between deformation and retrogression in blueschist metapelites of Tinos island (Greece) evidenced by chlorite-mica local equilibria. *Lithos* **63**, 41–66.

Perinçek, D. & Özkaya, İ. 1981. Tectonic evolution of the northern margin of Arabian plate. *Yerbilimleri Dergisi, Journal of the Earth Sciences Application and Research Centre of Hacettepe University* **8**, 91–101 [in Turkish with English abstract].

Rigo de Righi, M. & Cortesini, A. 1964. Gravity tectonics in foothills structure belt of southeast Turkey. *Bulletin of the American Association of Petroleum Geology* **48**, 1911–1937.

Rimmelé, G., Jolivet, L., Oberhänsli, R. & Goffé, B. 2002. Deformation history of the high-pressure Lycian Nappes and implications for tectonic evolution of SW Turkey. *Tectonics* **22**, 1–20.

Rimmelé, G., Parrra, T., Goffé, B. Oberhänsli, R., Jolivet, L. & Candan, O. 2005. Exhumation paths of high-pressure–low-temperature metamorphic rocks from the Lycian Nappes and the Menderes Massif (SW Turkey): a multi-equilibrium approach. *Journal of Petrology* **46**, 641–669.

Rolland, Y., Billo, S., Corsini, M., Sosson, M. & Galoyan, G. 2008. Blueschists of the Amassia-Stepanavan Suture Zone (Armenia): linking Tethys subduction history from E-Turkey to W-Iran. *International Journal of Earth Sciences* **98**, 533–550.

Ruffet, G., Féraud, G., Ballèvre, M. & Kienast, J.R. 1995. Plateau ages and excess argon in phengites: an ^{40}Ar-^{39}Ar laser probe study of Alpine micas (Sesia Zone, Western Alps, northern Italy). *Chemical Geology* **121**, 327–343.

Şengör, A.M.C. & Yilmaz, Y. 1981. Tethyan evolution of Turkey, a plate tectonic approach. *Tectonophysics* **75**, 181–241.

Şengör, A.M.C., Özeren, S., Genç, T. & Zor, E. 2003. East Anatolian high plateau as a mantle-supported, north–south shortened domal structure. *Geophysical Research Letters* **30**, 8045, DOI: 10.1029/2003GL017858.

Sherlok, S, Kelley, S., Inger, S., Harris, N. & Okay, A. 1999. ^{40}Ar-^{39}Ar and Rb-Sr geochronology of high-pressure metamorphism and exhumation history of the Tavşanlı Zone, NW Turkey. *Contributions to Mineralogy and Petrology* **137**, 46–58.

Sherlok, S. & Kelley, S. 2002. Excess argon evolution in HP-LT rocks: a UVLAMP study of phengite and K-free minerals, NW Turkey. *Chemical Geology* **182**, 619–636.

Sosson, M., Rolland, Y., Müller, C., Danelian, T., Melkonyan, R., Kekelia, S., Adamia, S., Babazadeh, V., Kangarli, T., Avagyan, A., Galoyan, G. & Mosar, J. 2010. Subductions, obduction and collision in the Lesser Caucasus (Armenia, Azerbaijan, Georgia), new insights. *In*: Sosson, M., Kaymakci, N., Stephenson, R.A., Bergerat, F. & Starostenko, V. (eds), *Sedimentary Basin Tectonics from the Black Sea and Caucasus to the Arabian Platform*. Geological Society, London, Special Publications **340**, 329–353.

Spear, F. & Cheney, J. 1989. A petrogenetic grid for pelitic schists in the system SiO_2-Al_2O_3-FeO-MgO-K_2O-H_2O. *Contributions to Mineralogy and Petrology* **101**, 149–164.

Sungurlu, O. 1974. VI. Bölge kuzey sahalarının jeolojisi [Geology of VIth northern area]. *Türkiye İkinci Petrol Kongresi, Abstracts*, Ankara, 85–107.

Theye, T., Seidel, E. & Vidal, O. 1992. Carpholite, sudoite and chloritoid in low-grade high-pressure metapelites from Crete and the Peloponnese, Greece. *European Journal of Mineralogy* **4**, 487–507.

Tolun, N. 1953. Contributions à l'étude géologique des environs du sud et sud-ouest du Lac de Van. *Mineral Research and Exploration Institute Bulletin* **44/45**, 77–112.

Vidal, O., Goffé, B., Bousquet, R. & Parra, T. 1999. Calibration and testing of an empirical chloritoid-chlorite Mg-Fe exchange thermometer and thermodynamic data for daphnite. *Journal of Metamorphic Geology* **17**, 25–39.

Vidal, O. & Parra, T. 2000. Exhumation paths of high-pressure metapelites obtained from local equilibria for chlorite-phengite assemblages. *Geological Journal* **35**, 139–161.

Vidal, O. & Theye, T. 1996. Comment on 'Petrology of Fe-Mg-carpholite-bearing metasediments from NE Oman'. *Journal of Metamorphic Geology* **14**, 381–386.

Villa, I.M., 1998. Isotopic closure. *Terra Nova* **10**, 42–47.

Wiederkehr, M., Bousquet, R., Schmid, S. M. & Berger, A. 2008. From subduction to collision: thermal overprint of HP/LT meta-sediments in the north-eastern Lepontine Dome (Swiss Alps) and consequences regarding the tectono-metamorphic evolution of the Alpine orogenic wedge. *Swiss Journal of Geosciences* **101**, 127–155.

Yiğitbaş, E. & Yilmaz, Y. 1996. New evidence and solution to the Maden complex controversy of the Southeast Anatolian orogenic belt (Turkey). *Geologische Rundschau* **85**, 250–263.

Yilmaz, O., Michel, R., Valette, Y. & Bonhomme, M.G. 1981. Réinterpétation des données isotopiques Rb-Sr obtenues sur les métamorphites de la partie méridionale du massif de Bitlis (Turquie). *Bulletin des Sciences Géologique Strasbourg* **34**, 59–73.

Yilmaz, Y. 1978. Gevaş (Van) dolayında Bitlis Masifi/ofiyolit ilişkisi [Bitlis Massif/ophiolite relationship in Gevaş (Van) region]. *Türkiye. 4. Petrol Kongresi Bildiriler Kitabı*, 83–93.

Yilmaz, Y. 1993. New evidence and model on the evolution of the southeast Anatolian orogen. *Bulletin of the Geological Society of America* **105**, 252–271.

York, D. 1969. Least square fitting of a straight line with correlated errors. *Earth and Planetary Science Letter* **5**, 320–324.

Zor, E., Sandvol, E., Gürbüz, C., Türkelli, N., Seber, D. & Barazangi, M. 2003. The crustal structure of the East Anatolian plateau (Turkey) from receiver functions. *Geophysical Research Letters* **30**, 8044.